JOURNAL OF MATERIALS SCIENCE 10 (1975) 621–632

Dynamic effects in the impact testing of brittle materials

P. W. McMILLAN, J. R. TESH*
Department of Physics, University of Warwick, Coventry, Warwickshire, UK

The results of an experimental investigation of impact failure in a glass, a glass-ceramic and two conventional ceramics are reported. This revealed the occurrence of complex dynamic effects during impact as a result of vibrations induced in the test specimen. These effects were studied by using strain gauges fitted to the impacter and the specimen. To aid understanding of the observations, computer simulation of impact behaviour was undertaken and the results were compared with the experimental data. Conclusions are drawn concerning the design and limitations of impact testing machines of the pendulum type for investigating impact failure of brittle materials. The value of instrumentation of the pendulum and of computer calculations of the type described in this paper is emphasized.

1. Introduction

The possibility of failure as a result of impact imposes severe constraints on engineering design in cases where it is necessary to employ brittle materials (e.g. ceramics, glasses). Despite the technological importance of impact failure, the basic features are not well understood and the methods used to measure "impact strength" leave much to be desired.

Standard tests such as the Charpy and Izod tests, in which the energy lost by a heavy pendulum in breaking a specimen rod is measured, provide a means of comparing materials subjected to identical impacts, but Charpy test results cannot be converted to equivalent Izod values and vice versa and it is not possible to scale the results for varying specimen dimensions. Impact strengths measured in this way cannot, therefore, be considered a fundamental property of the material and the results must be applied with great caution, especially in situations where the type of impact or the component shape and dimensions differ greatly from those used in the test. Factors that influence the type of impact include the impact velocity, the hardness and shape of the impacter (controlling the area of contact), the elastic stiffness of both the impacter and supports, the amount of mechanical damping in these members, the atmosphere and the temperature.

Impact tests are usually carried out either to obtain information about the impact behaviour of a material *per se* or to check predictions of impact behaviour extrapolated from data obtained in static tests. The tests may, however, be intended to obtain information about more general properties, but this is not particularly satisfactory owing to the difficulty of interpreting the results of the test. The simplicity of the impact test, however, is sometimes taken as a justification for its use where a more fundamental form of test would be difficult or expensive to carry out. Typical examples are the estimation of the work of fracture from an impact energy value and the calculation of fracture toughness from the peak load in an instrumented impact test.

In evaluating these methods of using impact tests it is useful to consider how they differ from the static test carried out in a hard testing machine with a driven cross-head.

(a) In an impact test the applied forces on the specimen result from the deceleration of the pendulum. Thus the displacement rate cannot be kept constant whereas in a hard machine the cross-head moves at a constant rate; it could be considered to be a slowly moving impact pendulum of near infinite mass. A traditional impact test, however, cannot be carried out with a very massive pendulum because the energy loss during impact would be negligible and, therefore, virtually impossible to measure.

(b) Impact tests are usually carried out a

*Present address: King Edward's Five Ways School, Scotland Lane, Birmingham.

velocities around 1 m sec^{-1} or greater, whereas static tests use very low velocities. The high rates of loading during impact mean that the inertia of the specimen cannot be neglected; vibrations occur and the simple static formulae for the stress distribution in the specimen cannot be used.

Clearly, it would be of great value if the results of static tests could be used to predict the behaviour of a material under various types of impact but the inertial forces make the interpretation of impact results in terms of more basic material properties extremely difficult. To provide a basis for progress in this direction it was considered worthwhile to undertake an investigation into effects arising during impact both from the theoretical and experimental viewpoints.

2. The theory of impact

Because of the complexity of impact processes, approximations must inevitably be used in order to produce a theory which is of practical use. A very useful simple theory suggested by Cox [1] or Goldsmith [2] is worth considering. The specimen is considered as a mass

$$m = \frac{17}{35} m_l \tag{1}$$

mounted on a spring of stiffness

$$s = \frac{3\pi Y d^4}{4l^3}, \tag{2}$$

where Y, d and l are the Young's modulus, diameter and length between the supports of the specimen, and m_l is the mass of that part of the specimen between the supports. During the impact the pendulum and specimen are considered to move together, so that the force-time curve is half a sine wave, and the impact duration is

$$\tau = \pi \left(\frac{m_h + m}{s} \right)^{\frac{1}{2}} \tag{3}$$

where m_h is the mass of the pendulum. This implies a perfectly inelastic collision between pendulum and specimen, which does not agree with experiment as far as brittle materials are concerned. However, by assuming that the specimen mass is small compared with that of the pendulum, we can avoid this problem and say that the maximum displacement, U_m, of the specimen and pendulum is

$$U_m = V_i (m_h/s)^{\frac{1}{2}}, \tag{4}$$

where V_i is the impact velocity. In this model the specimen is assumed to bend to the static equilibrium shape, so we can write the maximum tensile stress due to bending as

$$\sigma = \frac{8lsU}{\pi d^3} \tag{5}$$

and the total elastic energy as

$$E = \tfrac{1}{2} s U^2. \tag{6}$$

In order to improve on the Cox model a series of computer programs have been developed on the basis of less drastic assumptions. The computer is needed because the solutions involve integrals which cannot be evaluated explicitly.

The first program, "IMPACT ONE" was nearest to Cox's model.*In this the specimen and pendulum are allowed to move independently and the force between them is a Hertzian elastic force:

$$\begin{aligned} F &= k(U_h - U)^{1.5} \quad U_h > U \\ F &= 0 \qquad\qquad\quad U_h < U. \end{aligned} \tag{7}$$

Here U is the forward displacement of the specimen and U_h is that of the pendulum. The pendulum is treated as a point mass without vibrations and the specimen is treated as in Cox's model.

In these programs the impact is divided into a series of small time intervals during which the force is kept constant and the motion under its influence of the specimen and striker is calculated. From their final positions at the end of the interval a new force is calculated, and this is used for the next period.

The most useful program was "IMPACT TWO"*which is similar to "IMPACT ONE" except that the specimen motion is correctly calculated from the Bernoulli-Euler equation of simple beam theory (Timoshenko [3], Goldsmith [2]). If D_j represents the convolution integral

$$D_j = \int_0^t F(\tau) \sin \omega_j (t - \tau) \mathrm{d}\tau, \tag{8}$$

where t and τ represent time and ω_j is one of the normal mode vibration frequencies of the specimen, then the displacement of the specimen centre is

$$U(t) = \frac{1}{\rho A l} \sum_{j = 1, 3, 5 \ldots}^{\infty} \frac{D_j}{\omega_j}, \tag{9}$$

*Supplementary Publication, British Library Lending Division, SUP 90011, 5pp.

where ρ is the specimen density, A the cross-sectional area, and l the length between the supports. The total elastic strain energy is

$$E(t) = \frac{1}{\rho A l} \sum_{j=1,3,5\ldots}^{\infty} D_j^2, \qquad (10)$$

and the greatest tensile stress on the back face of the specimen is

$$\sigma(t) = \frac{dE^{\frac{1}{2}}}{l(\rho A I)^{\frac{1}{2}}} \sum_{j=1,3,5\ldots}^{\infty} D_j . \qquad (11)$$

This is a theoretical calculation, and it must not be confused with the problem of converting experimentally observed forces into stresses. The mathematics is the same but the starting data are different.

Further improvements on these programs have been developed. These chiefly involved a more accurate representation of the specimen vibrations, and an allowance for the effect of the pendulum vibrations. These greatly increased the complexity of the program without much change in the results, so they will not be considered further.

3. Experimental methods

3.1. Preliminary impact and static strength tests

A simple impact machine of the general design illustrated in Fig. 1 was constructed. In this the impact was generated by a horizontally swinging Dural arm which was driven by a compressed helical spring released by a trigger mechanism.

Specimens in the form of rods about 6 cm long were positioned against hardened steel pins 4.5 cm apart. When the trigger of the machine was released the Dural arm swung through 180° causing a hammer mounted on the end to strike the centre of the specimen rods. Interchangeable hammers were provided, allowing different shapes and materials to be investigated.

The velocity of the arm before and after the impact was derived by illuminating the apparatus with a stroboscope lamp and recording the multiple image with a camera. Fig. 2 shows a typical result. In this way the energy absorbed as a result of the impact could be derived and it was also possible to follow the trajectories of the fragments of the broken specimen and thus to make an estimate of their kinetic energy. Allowance was made for the friction losses in the

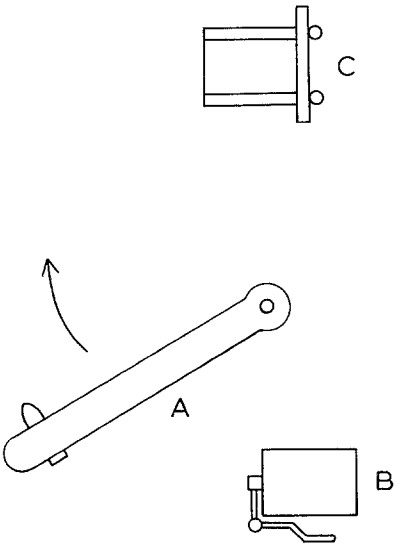

Figure 1 Layout of the impact testing machine.

machine when calculating the energy absorbed during impact. The apparatus was normally housed in a glove box to allow the tests to be carried out in dry nitrogen gas.

Several materials were selected for investigation as follows:

(a) Soda-lime silica glass rods 4.5 mm and 9 mm nominal diameters. These were tested in the as-received condition and also after an abrasion treatment which comprised rotating ten rods with approximately their own weight of silicon carbide powder for 30 min in a jar mill.

(b) Lithium alumino-silicate glass-ceramic rods in the unground condition (diameters 4 to 5 mm) and after surface grinding (diameters 4.00 $\pm$ 0.05 mm).

(c) 95% alumina ceramic rods surface ground to a diameter of 4.00 $\pm$ 0.05 mm.

(d) Electrical procelain rods surface ground to a diameter of 4.00 $\pm$ 0.05 mm.

In the case of the soda-lime-silica glass rods (group a), the effects of various pretreatments and storage conditions were studied. These included testing in the as-received condition, after storage in a desiccator, after storage in liquid nitrogen and after storage under distilled water. In the case of the last type of specimens some were tested while still wet while others were dried before testing in dry nitrogen.

For the other materials (groups b to d) testing was always on the as-received specimens in a dry nitrogen atmosphere.

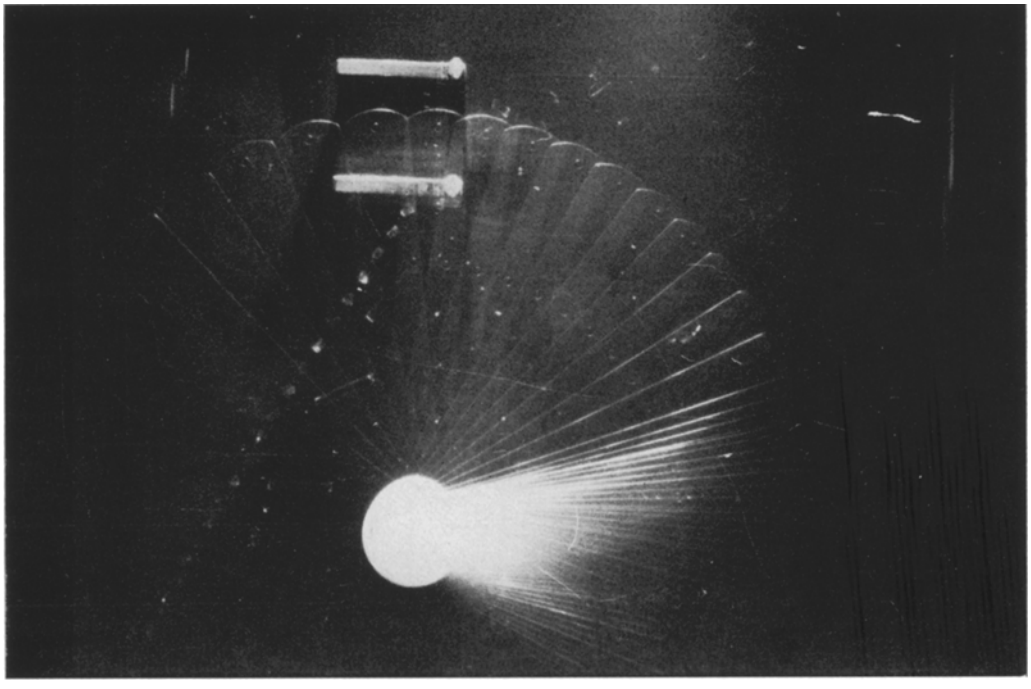

Figure 2 Photographic record of an impact test.

For comparison with the impact test results measurements of modulus of rupture were made using an "Instron" equipment with a three-point bending attachment. The specimens were supported on two steel rods 4 cm apart and loaded by a central rod driven downwards at 0.05 mm min^{-1}.

The atmosphere during testing was controlled, as far as possible by enclosing the specimen and loading arrangement in a dry-nitrogen filled polythene bag. Sets of specimens having similar pretreatments and surface conditions to those employed for the impact studies were tested.

3.2. Fractography of glasses and glass-ceramics

It was considered useful to examine the fracture surfaces of glass and glass-ceramic specimens in some detail. For examination in a scanning electron microscope, the fracture surfaces were coated with a thin film of gold-palladium alloy by an evaporation technique.

3.3. Instrumental impact tests

Following the preliminary investigation it was realized that the derivation of force-time curves for the period of immediately following the contact of the impacter with the specimen rod would make an important contribution to the understanding of the processes taking place.

For this reason the impact testing machine described earlier was modified by cementing a strain gauge (Ether Engineering Ltd, type 3A-1A-350P) to the side of the striker with Araldite strain gauge cement. This was connected in series with a wire resistor of the same magnitude and two 9 V batteries. The input of an oscilloscope was connected to the gauge at the resistor side. Calibration was carried out statically by placing the striker against a steel rod and hanging weights from it using a simple pulley arrangement.

Using this method, force-time curves were obtained for 4.5 and 9 mm diameter soda-lime-silica glass rod specimens, using a span of 45 mm and varying the velocity of the impacter.

The results of these investigations suggested that a modified form of impact test should be studied. Accordingly, it was decided to use a ballistic pendulum as a means of producing the impact since this would eliminate problems due to vibration of the swinging arm encountered with the first method. A steel bob of mass 55 g having a rounded nose was suspended by four

TABLE I Results of impact tests

Material	Surface treatment and test conditions	Number of specimens	Nominal diameter (mm)	Velocity of impacter ($msec^{-1}$)	Energy absorbed E (mJ)	Coefficient of variation (%)	E/E_s
Glass	As-received	13	4.5	0.800	37	17	3.8
Glass	As-received	9	4.5	1.043	40	28	4.2
Glass	As-received	10	4.5	1.260	48	30	5.0
Glass	Abraded, dry	10	4.5	0.465	8.6	24	4.1
Glass	Abraded, dry	10	4.5	0.792	9.3	30	4.4
Glass	Abraded, liquid nitrogen	9	4.5	0.450	8.1	34	—
Glass	Abraded, wet	10	4.5	0.478	8.4	16	4.6
Glass	Abraded, dry	9	9	1.108	57	25	17
Glass	Abraded, dry	9	9	1.303	63	35	19
Glass	Abraded, wet	9	9	1.292	68	29	23
Glass-ceramic	Ground, as-received	10	4.0	1.312	23	20	4.3
Alumina	Ground, as-received	10	4.0	0.853	21	16	6.2
Porcelain	Ground, as-received	10	4.0	0.497	15.1	6	3.2

TABLE II Results of modulus of rupture measurements

Material	Surface treatment	Number of specimens	Diameter (mm)	Modulus of rupture σ_s ($MN\ m^{-2}$)	Coefficient variation (%)
Glass	As-received	10	4.5	147	21
Glass	Abraded, wet and dried	10	4.5	68	8
Glass	Abraded, wet	10	4.5	68	8
Glass	As-received, dry	9	9	82	19
Glass	As-received, wet	10	9	105	28
Glass	Abraded, dry	10	9	42	10
Glass	Abraded, wet and dried	10	9	42	18
Glass	Abraded, wet	10	9	37	11
Glass-ceramic	Not ground, as-received	10	4.6	321	15
Glass-ceramic	Ground, as-received	10	4.0	138	8
Alumina	Ground, as-received	10	4.0	208	5
Porcelain	Ground, as-received	10	4.0	122	5

nylon cords 1 m long from a rigid frame. A strain gauge, calibrated in the manner described previously, was cemented onto the side of the bob. The rod specimens rested across two horizontal rails against steel pegs the position of which could be varied incrementally to give spans between 45 and 95 mm. The specimens were struck horizontally at their centres.

4. Results and discussion

4.1. Preliminary investigations

The results of the impact and static strength measurements are given in Tables I and II respectively. Two classes of specimens were so strong that they could not be broken with the impact machine. These were the 9 mm diameter glass rods in the as-received condition and the unabraded glass-ceramic rods. It is concluded that the impact energy for these specimens must be greater than about 200 mJ.

As expected, abrasion reduced both the mean modulus of rupture and the energy absorbed during impact failure and reduced the scatter of the results. The results in Table I also indicate that the energy absorbed during impact failure of the glass specimens increases with increasing velocity of the impacter and again this result is not unexpected, since the breaking strength of glass is known to depend on the rate of loading; with lower rates of loading the so-called static fatigue effect causes a reduction of strength. Comparison between the different materials is

not easy since different velocities of the impacter were used but the results indicate that the energy absorbed on impact is higher for abraded (ground) glass-ceramic and alumina than for abraded glass.

To form a basis of comparison between the results of the impact tests and the modulus of rupture results, it was decided to calculate the ratio between the energy absorbed during impact, E, and the strain energy stored in the specimens immediately before failure, E_S, calculated from the modulus of rupture results. This ratio is given in the last column of Table I.

The strain energy E_S was calculated as follows: assuming the rod fails when the surface stress reaches a critical value σ_S then in the static case the applied load to cause failure is given by simple beam theory:

$$Wg = \frac{\pi\sigma_S^2 d^3}{16l}, \tag{12}$$

where d is the specimen diameter, W the applied load, g the gravitational constant and $2l$ the length between the supports. The deflection δ, assumed to be small, is

$$\delta = \frac{32Wgl^3}{3\pi Yd^4}, \tag{13}$$

where Y is Young's modulus. Thus at the instant of fracture, the elastic energy is

$$E_S = \tfrac{1}{2}Wg\delta = \frac{16W^2g^2l^3}{3\pi Yd^4} = \frac{\pi\sigma_S^2 d^2 l}{48Y}. \tag{14}$$

It will be seen that for the 4.5 mm diameter glass specimens the ratio E/E_S is approximately constant at about 4 to 5 despite quite large variations in the values of σ_S the modulus of rupture and E the energy absorbed during impact failure. Also the ratios for the glass-ceramic, alumina and porcelain rods do not depart greatly from those observed for the glass specimens. In similar calculations on the results for glass rods, Haward [4] found ratios ranging from 1.3 to 1.8. The higher values found in the present work for the 4 to 4.5 mm diameter rods may be due to the use of a rather low loading rate in the static tests with the result that the measured values of σ_S were low owing to static fatigue effects. The values of the ratio E/E_S for the 9 mm diameter glass rods are very much higher than those for the thinner rods and possibly this is because the simple beam theory used in the calculations is not adequate for specimens having this diameter to length ratio. For such specimens, shear strain energy cannot be neglected and Equation 14 would no longer be valid.

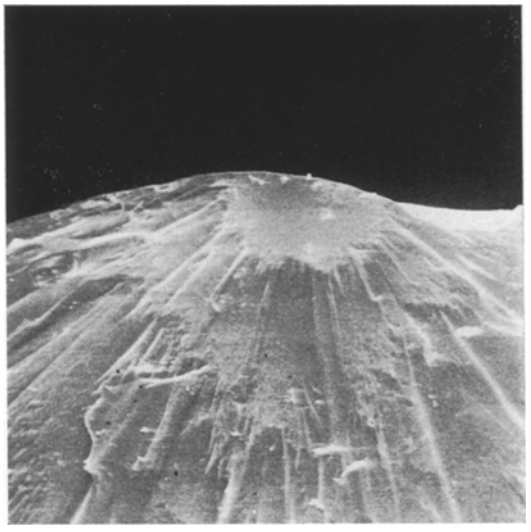

Figure 3 Fracture surface of a glass specimen (× 100).

4.2. Fractography of glasses and glass-ceramics

Fig. 3 shows the origin of fracture of a glass specimen at × 100 magnification. Levengood [5], Shand [6], Johnson and Holloway [7] and others have found empirically that the radius, r,

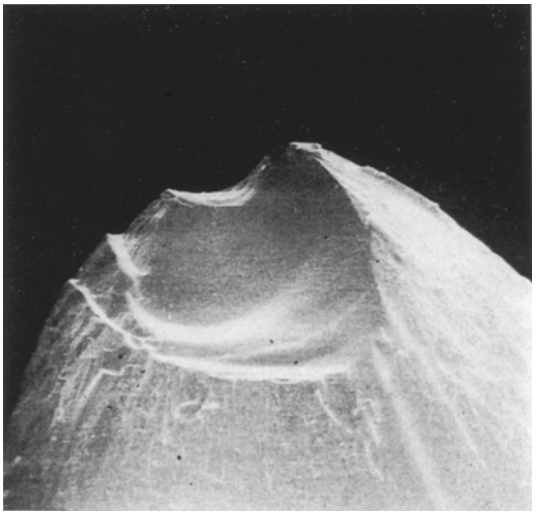

Figure 4 Fracture surface of a glass-ceramic specimen (× 100).

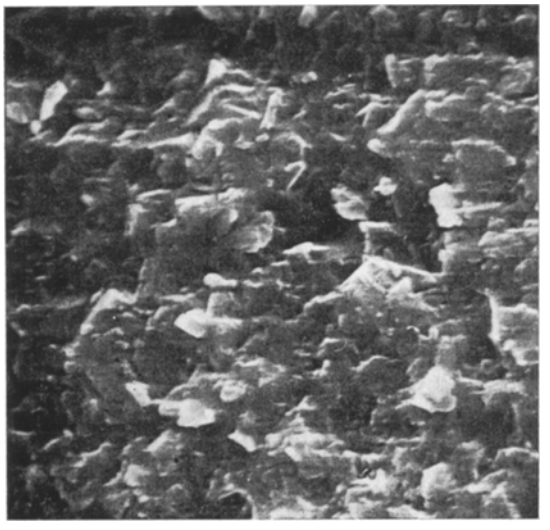

Figure 5 Fracture surface of a glass-ceramic specimen: smooth region (× 5000).

of this "mirror" region is related to the breaking stress σ by a relationship

$$\sigma\sqrt{r} = C\,, \qquad (15)$$

where C is characteristic of the material. For the soda-lime-silica glass used in these experiments, the value of C was found to be 2.2 ± 0.1 MN $m^{-3/2}$ (6.7 ± 0.4 kg $mm^{-3/2}$) which agrees well with the values found by other workers. The impacted specimens showed a range of mirror sizes which did not differ significantly from those in the static bend test and if Equation 15 can be used in the case of impact, this suggests that the breaking stresses during impact were similar to those in the static bend test.

The fracture surface of the glass-ceramic (Fig. 4) showed similar features to that of the glass in that there was a relatively smooth area around the presumed origin of the fracture surrounding the smooth area there was a "hackled" region. However, the smooth area was shown to be rough when a sufficient magnification was employed (Fig. 5) although the scale of roughening was possibly less than that in the hackle region (Fig. 6). The fracture surfaces in both regions show angular features suggesting that in some regions the crack tends to propagate through the residual intergranular glass phase. This type of fracture propagation may be one reason why the fracture toughness of glass-ceramics is higher than that of uncrystallised glass.

4.3. Instrumented impact tests

Contact force-time curves derived experimen-

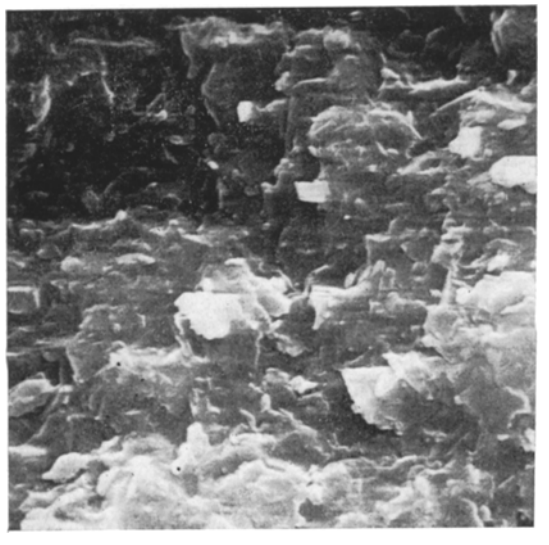

Figure 6 Fracture surface of a glass-ceramic specimen: hackle region (× 5000).

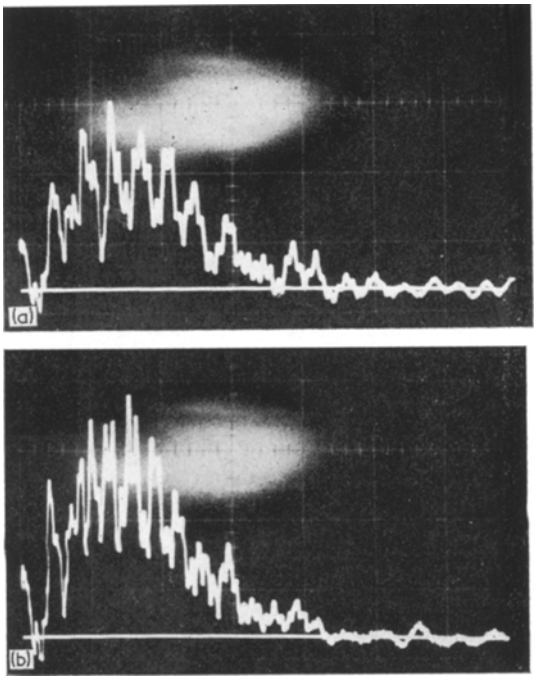

Figure 7 Contact force-time curves for 4.5 mm diameter glass rods; span 45 mm. Vertical scales 200 N per large division. Horizontal scales 400 μsec per large division. (a) Impact velocity 1.4 $msec^{-1}$. (b) Impact velocity 1.7 $msec^{-1}$. (c) Impact velocity 1.9 $msec^{-1}$.

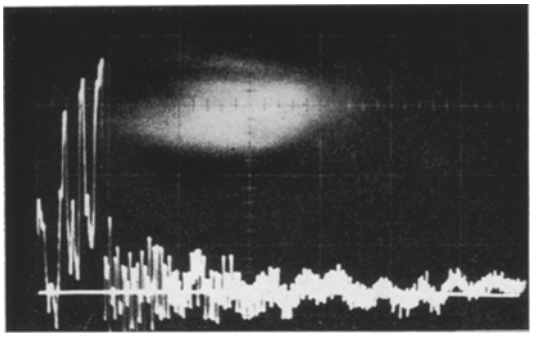

Figure 8 Contact force-time curve for 4.5 mm diameter glass rod when fracture occurred; span 45 mm. Vertical scale 200 N per large division. Horizontal scale 400 μsec per large division. Impact velocity 2.0 $msec^{-1}$.

tally for the 4.5 mm glass rod specimens are shown for different impact velocities in Fig. 7. It is seen that these are very complex though certain general features are apparent; the force rises fairly rapidly and then decays and the maximum pulse height scales approximately with the impact velocity.

An example of the trace obtained when the specimen fractured is given in Fig. 8. The force decreases rapidly on fracture but oscillations continue to be recorded after fracture due to vibrations set up in the striker and arm of the impact machine.

The results obtained for the 9 mm diameter glass rods were less complex as shown by Fig. 9 which give traces for unbroken specimens. Typical traces for specimens that fractured are given in Fig. 10. Again the maximum pulse height increases with increase of velocity of the impacter. For the specimen corresponding to Fig. 10a, failure occurred after about 70 μsec while the contact force was decreasing. The load then fell to zero in about 25 μsec. Using a higher impact velocity (Fig. 10b) the fracture occurred earlier, after about 50 μsec.

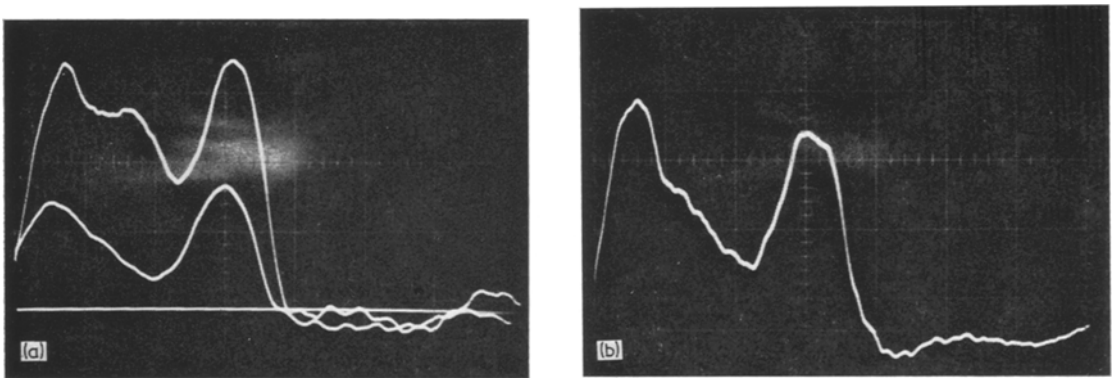

Figure 9 Contact force-time curves for 9.0 mm diameter glass rods; span 45 mm. (a) Vertical scale 200 N per large division. Horizontal scale 100 μsec per large division. Impact velocities 1.3 and 0.9 $msec^{-1}$. (b) Vertical scale 500 N per large division. Horizontal scale 100 μsec per large division. Impact velocity 2.3 $msec^{-1}$.

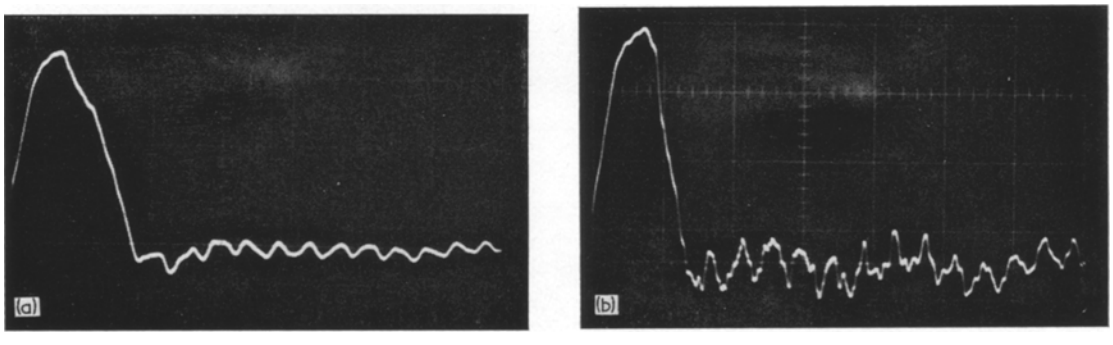

Figure 10 Contact force-time curves for 9 mm diameter glass rods when fracture occurs; span 45 mm. Vertical scales 500 N per large division. Horizontal scales 100 μsec per large division. (a) Impact velocity 2.1 $msec^{-1}$. (b) Impact velocity 2.3 $msec^{-1}$.

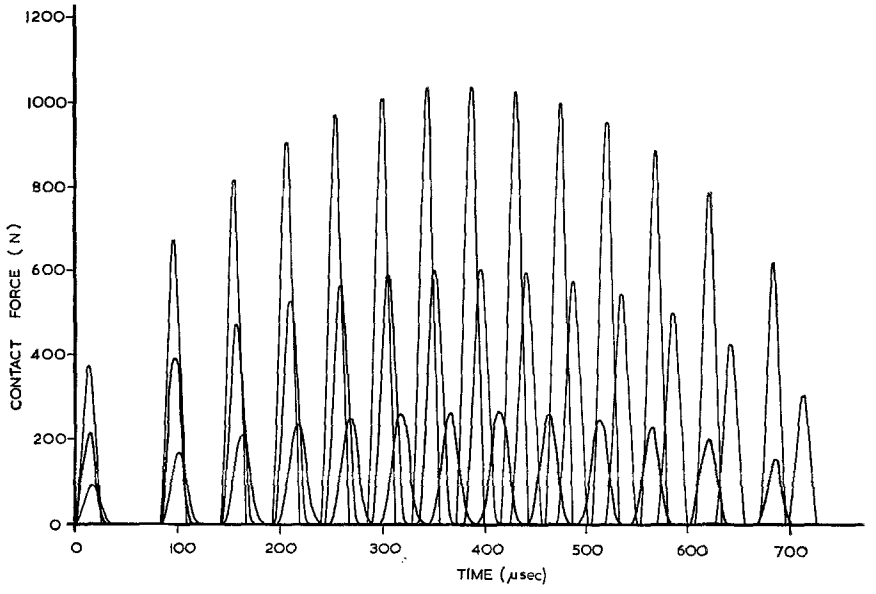

Figure 11 Computed contact force-time curves for 4.5 mm diameter glass rods; span 45 mm: "IMPACT ONE".

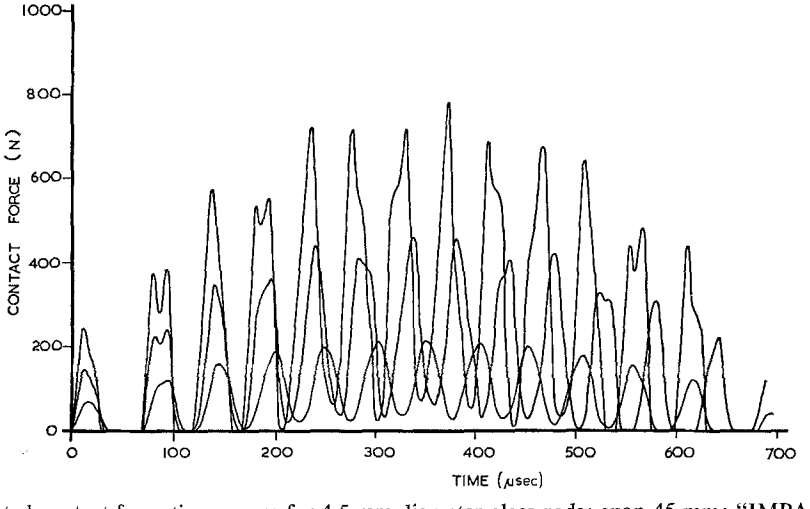

Figure 12 Computed contact force-time curves for 4.5 mm diameter glass rods; span 45 mm: "IMPACT TWO".

The results obtained in the foregoing experiments were compared with computer generated contact force-time curves derived using the "IMPACT ONE" and "IMPACT TWO" programs described in Section 2.

Fig. 11 shows computed curves for 4.5 mm diameter glass rods for three impact velocities: 0.8, 1.6 and 2.5 m sec^{-1}, according to "IMPACT ONE". Although the curves are complex, they are considerably less so than the experimental traces. The points of agreement between the experimental and theoretical traces are that the maximum pulse height increases with increase of impact velocity and the durations of the impact (about 800 μsec) also agree fairly well.

Curves for the three impact velocities derived using the "IMPACT TWO" program are given in Fig. 12. These are more complex than those given by the "IMPACT ONE" program but apart from the overall similarities, they do not reproduce the experimental traces very satisfactorily. The results of similar computations for the 9 mm diameter rods are shown in Fig. 13. Although these reproduce some of the general

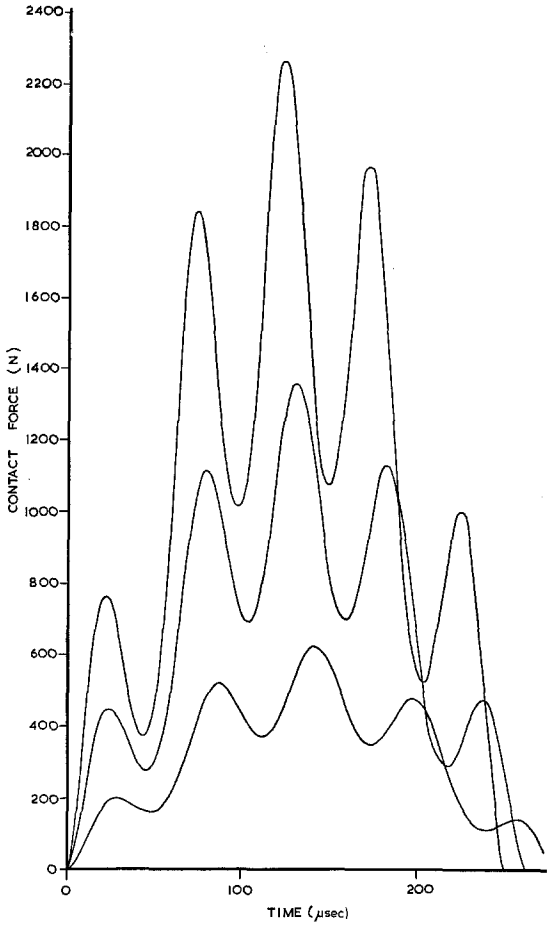

Figure 13 Computed contact force-time curves for 9 mm diameter glass rods; span 45 mm: "IMPACT TWO".

features of the experimental traces, the detailed agreement is less than satisfactory.

On the basis of these results it was concluded that the failure to obtain agreement between the experimental results and the theoretical predictions was due at least in part to deficiencies of the impact testing machine. In particular, oscillations in the striker and the swinging arm were thought to introduce undesirable complexities into the recorded traces. For this reason, trials were undertaken with the ballistic pendulum; typical results are given in Figs. 14 and 15 for 4.5 mm diameter glass rods and in Fig. 16 for 9 mm diameter rods. Also given in Fig. 15 are stress-time curves derived from a strain gauge cemented to the rod specimens. The upper curve in Fig. 14 is for a specimen that survived the impact and the lower curve is for a specimen that failed. Similarly, in Fig. 16 a comparison between a specimen that survived (upper curve) and one that failed (lower curve) is given.

The agreement between these experimental results and the theoretical prediction is good, especially in the case of the 9 mm diameter rods where the detailed features of the traces agree closely.

It is interesting to note that the traces of specimen stress, given in Fig. 14, are affected much less than the contact force by the details of the impact and they approximate to the half sinusoid predicted by the ideas of Cox.

From the theoretical and experimental studies undertaken it is clear that complex phenomena are involved in the impact testing. The interpretation of an impact test involves two stages. First the applied loads and displacements must be converted into the more physically meaningful stress and strain distributions (as a function of time); secondly these stresses and strains must be related to the failure behaviour.

In a static test the same stages are used, but the first conversion is a simple application of geometrical principles. In the dynamic case the

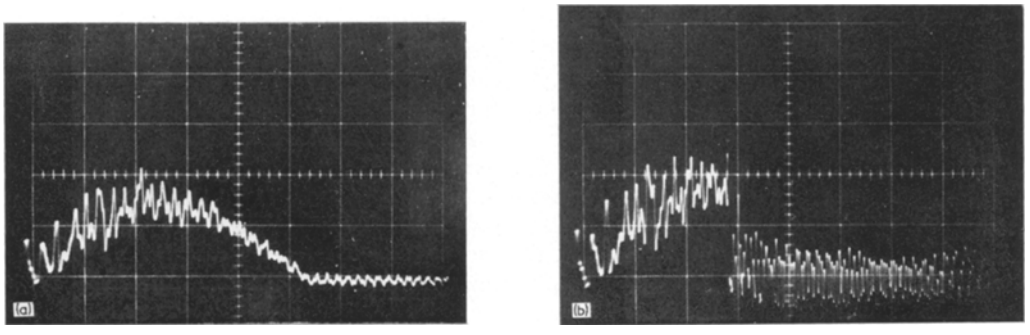

Figure 14 Contact force-time curves for 4.5 mm glass rods; span 45 mm. (a) Impact velocity 0.58 $msec^{-1}$. (b) Impact velocity 0.74 $msec^{-1}$.

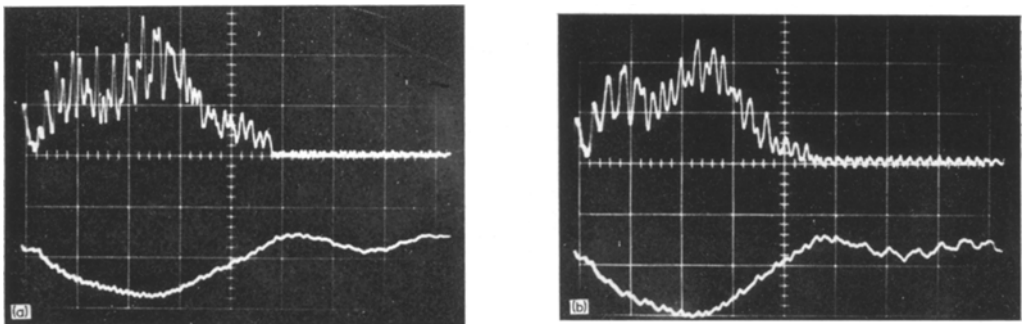

Figure 15 Contact force-time curves and tensile stresstime curves for 4.5 mm diameter glass rods; span 45 mm. (a) Vertical scales: force, 100 N per large division tensile stress, 40 MN m^{-2} per large division. Impact velocity 0.27 $msec^{-1}$. (b) Vertical scales: force, 200 N per large division tensile stress 100 MN m^{-2} per large division. Impact velocity 0.43 $msec^{-1}$.

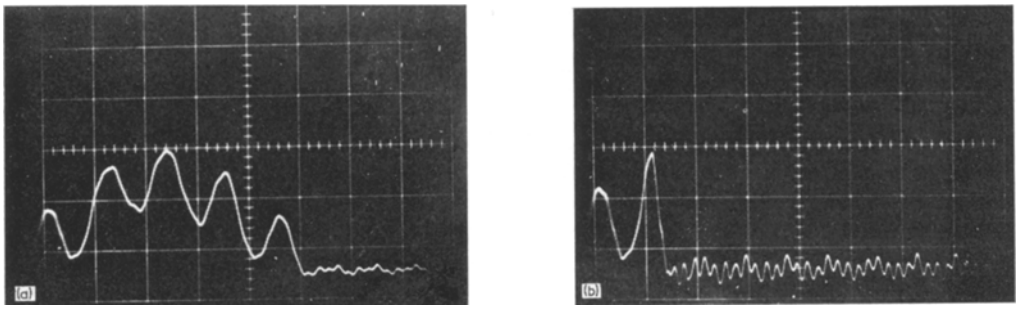

Figure 16 Contact force-time curves for 9 mm diameter glass rods; span 45 mm. Vertical scales 1000 N per large division. Horizontal scales 100 μsec per large division. (a) Impact velocity 2.3 $msec^{-1}$. (b) Impact velocity 2.6 $msec^{-1}$.

addition of the inertial forces makes the process very complex.

For the test used in the present work–a central lateral impact on a bar supported at the ends – the equations have been worked out as part of the program "IMPACT TWO". The stress distribution at a given instant depends not only on the instantaneous applied force, but on the complete force-time history of the impact, and the calculation depends on a knowledge of Young's modulus and on the assumptions of simple beam theory. Because of this the calculation breaks down when the specimen ceases to be elastic. Moreover, it is not possible to measure a local stress directly. With an elastic specimen one can measure the strain and convert it to stress, and this method can be used to check the calculations, but when the specimen begins to yield or break it has not been possible to obtain a value for the stress by either calculation or experiment. The problem of obtaining dynamic stress-strain curves for materials which yield or crack before failure is, therefore, very difficult. The present work has, therefore, concentrated on measuring the breaking stress in simple elastic-brittle materials.

Because of the complexity of the computer calculations used in this work, and their limited applicability, it is interesting to compare the results with the very simple ideas outlined at the beginning of Section 2. For the case of glass rods of diameter 4.5 mm, and span between the supports 45 mm the simple theory predicts a maximum deflection of the specimen of 0.59 mm, whereas "IMPACT TWO" predicts a maximum deflection of 0.67 mm, oscillating by about 3% below this. Similarly the simple theory predicts a maximum surface tensile stress of 560 MN m^{-2}, whereas "IMPACT TWO" predicts 640 MN m^{-2}, oscillating by 12%. The simple theory predicts a maximum elastic energy of 0.13 J, whereas "IMPACT TWO" predicts 0.17 J, oscillating by about 10%. This gives some ideas of the errors in the simple calculation.

5. Conclusions

(1) In designing an impact pendulum machine care must be taken to concentrate the pendulum weight in the bob, and keep the pivot and arm as light as possible. The ballistic pendulum is the easiest way of doing this.

(2) Instrumentation of the pendulum with strain gauges, together with computer calculations of the type described in this paper, provides warning of unsatisfactory tests and provides a great deal of useful additional information about the impact processes.

(3) For a simple elastic-brittle material the oscilloscope traces may be interpreted to obtain the loading history and failure stress at the flaw.

(4) Further work is required on instrumented pendulum equipped to measure the traditional absorbed energy measure of impact strength, to obtain sufficient data to allow a comparison of the methods to be made.

(5) Further work is required to find a way of obtaining a high speed stress strain curve from an instrumented impact test, for non-brittle materials.

(6) Because of the irregular nature of the stress pulses produced in the pendulum test, it is not suitable for evaluating the effect of fast loading rates on the growth of brittle flaws. Work is required to devise a test which produces a stress pulse of smooth profile.

Acknowledgement

The authors wish to thank the National Physical Laboratory for financial support.

References

1. E. COX, *Trans. Camb. Phil. Soc.* **9** (1849) 73.
2. W. GOLDSMITH, "Impact" (Arnold, 1960) p. 53.
3. S. TIMOSHENKO, "Vibration Problems in Engineering", 3rd Edn. (Wiley, 1966) p. 411.
4. R. N. HAWARD, *J. Soc. Glass Technol.* **28** (1944) 5.
5. W. C. LEVENGOOD, *J. Appl. Phys.* **29** (1958) 820.
6. E. B. SHAND, *J. Amer. Ceram. Soc.* **42** (1959) 474.
7. J. W. JOHNSON and D. G. HOLLOWAY, *Phil. Mag.* **14** (1966) 731.

Received 26 September and accepted 5 November 1974.